



1 **High contribution of anthropogenic combustion sources to**
2 **atmospheric inorganic reactive nitrogen in South China**
3 **evidenced by isotopes**

4
5 Tingting Li^{1,2,4}, Jun Li^{*1,2}, Zeyu Sun^{3,4}, Hongxing Jiang¹, Chongguo Tian³, Gan Zhang^{1,2}

6
7 ¹State Key Laboratory of Organic Geochemistry and Guangdong province Key Laboratory of Environmental
8 Protection and Resources Utilization, Guangdong-Hong Kong-Macao Joint Laboratory for Environmental
9 Pollution and Control, Guangzhou Institute of Geochemistry, Chinese Academy of Sciences, Guangzhou, 510640,
10 China

11 ²CAS Center for Excellence in Deep Earth Science, Guangzhou 510640, P. R. China

12 ³Yantai Institute of Coastal Zone Research, Chinese Academy of Sciences, Yantai 264003, P. R. China

13 ⁴University of Chinese Academy of Sciences, Beijing 100049, P. R. China

14 **Correspondence to:* Jun Li (junli@gig.ac.cn)

15
16 **Abstract:** Due to the intense release of reactive nitrogen (Nr) from anthropogenic activity, the
17 source layout of atmospheric nitrogen aerosol has changed. The inorganic nitrogen (NH₄⁺ and
18 NO₃⁻) was essential part of atmospheric nitrogen aerosol and accounted for 69%. To
19 comprehensively clarify the level, sources, and environmental fate of NH₄⁺ and NO₃⁻, their
20 concentrations and stable isotopes (δ¹⁵N) in fine particulate matters (PM_{2.5}) were measured in
21 a subtropical megacity of South China. N-NH₄⁺ and N-NO₃⁻ contributed 45.8% and 23.2% to
22 total nitrogen (TN), respectively. The source contributions of NH₄⁺ and NO₃⁻ were estimated
23 by δ¹⁵N, which suggested that anthropogenic combustion activities including coal combustion,
24 biomass burning, and vehicles were dominant sources. Especially, biomass burning was the
25 predominant source of NH₄⁺ (27.9%). Whereas, coal combustion was the dominant source of
26 NO₃⁻ (40.4%). This study emphasized the substantial impacts of human activities on inorganic
27 Nr. With the rapid development of industry and transportation, nitrogen emissions will be even
28 higher. The promotion of clean energy and efficient use of biomass would help reduce nitrogen
29 emissions and alleviate air pollution.



30 1. Introduction

31 Nitrogenous aerosols are ubiquitous in environment and play an important role as
32 nutrients in ecosystems(Bhattarai et al., 2019). With the massive combustion of fossil fuels and
33 the development of livestock, the proportion of TN in particulate matter (PM) ranges from 1.2%
34 to 17.0% and has shown a rapid increase in the last few decades(Bhattarai et al., 2019;
35 Galloway et al., 2004; Holland et al., 1999). Mostly nitrogenous aerosols formed from
36 atmospheric Nr will be deposited into terrestrial and aquatic ecosystems(Huang et al., 2015).
37 Excessive external nitrogen deposition accelerates nitrogen loss in soil, decreases species
38 diversity, disturbs terrestrial ecosystems, and leads to eutrophication in aquatic
39 ecosystems(Breemen, 2002; Wedin and Tilman, 1996; Yang et al., 2015). Furthermore,
40 nitrogenous aerosols have adverse impacts on the climate, air quality, and human
41 health(Bhattarai et al., 2019; Song et al., 2021).

42 N-NO₃⁻ and N-NH₄⁺ as inorganic Nr are dominant species in deposition of nitrogen(Zhu
43 et al., 2015). N-NH₄⁺ was the highest in nitrogen deposition, and NH₄⁺ was gradually
44 considered to be an important component of secondary inorganic aerosols (SIA)(Sun et al.,
45 2021). NH₃, precursor of NH₄⁺, is a vital atmospheric alkaline gas, which can participate in
46 nucleation to promote the new particles generation, and can react with acid gas to produce
47 ammonium sulfate and ammonium nitrate(Dunne et al., 2016; Fu et al., 2017). The excessive
48 NH₃ emission from anthropogenic sources will partially offset the benefits of reducing SO₂ and
49 NO_x and trigger urban haze in China(Sun et al., 2021; Meng et al., 2018; Pan et al., 2018). In
50 many urban environments, NO₃⁻ has replaced sulfate as the component with the highest
51 proportion in SIA. NO_x, precursors of NO₃⁻, are also closely related to the formation of
52 atmospheric oxidant and exert important effects on atmospheric oxidation. In addition,
53 NH₄NO₃ in PM plays an increasingly important role in promoting the formation of sulfate and
54 organic matter, and has profound effect on the physical and chemical properties of PM(Liu et
55 al., 2021; Liu et al., 2020; Hodas et al., 2014). Therefore, to mitigate the nitrogen deposition
56 and air pollution, the control of NH₄⁺ (NH₃) and NO₃⁻ (NO_x) should not be neglected.

57 Considerable efforts have been made to comprehensive understand budget of atmospheric
58 NH₄⁺ and NO₃⁻. δ¹⁵N is effective to quantify sources contribution of nitrogenous species(Elliott



59 et al., 2007). The anthropogenic combustion sources (combustion of coal, biomass, and
60 gasoline) play a key role in the emission of NO_3^- (NO_x) in many regions of China suggested
61 by $\delta^{15}\text{N}$ (Zong et al., 2020), which also have large effects on NH_3 . NH_3 is released by
62 agricultural source (agricultural activity and livestock) and non-agricultural source (fossil fuel
63 combustion and vehicle)(Bhattarai et al., 2019). Previous study showed that agricultural source
64 was the dominant source (80%-90%) of NH_3 in China(Kang et al., 2016). However, NH_3
65 emissions from agricultural source have been reduced due to intensive farming and efficient
66 fertilization(Wang et al., 2022). Combustion sources were gradually becoming dominant
67 sources of urban NH_3 in recent years verified by the methods of emission inventory and
68 $\delta^{15}\text{N}$ (Xiao et al., 2020; Meng et al., 2017). Especially, the incomplete burning of biomass leads
69 to massive NH_3 emission and is gradually to be the second largest non-agricultural source of
70 NH_3 (Yu et al., 2020), which may be responsible for the lag of the decline in air pollutants
71 deposition behind the reduction in emission of precursors(Zhao et al., 2022b). In addition, the
72 super clean emission of coal-fired power plant and strict emission standards of vehicles will
73 change the source layout of NH_4^+ and NO_3^- . Selective catalytic reduction technology equipped
74 with vehicles and industrial boiler reduces NO_x but increases NH_3 emissions(Meng et al., 2017;
75 Pan et al., 2016). The occurrence of haze in North China was closely related to NH_3 emissions
76 from combustion sources(Pan et al., 2018). NH_4^+ and NO_3^- are the main components of SIA
77 and play a vital role in the formation of secondary aerosol(Meng et al., 2017), so it is necessary
78 to revisit their sources.

79 Nr emissions from densely populated subtropical areas increased rapidly with the highly
80 development of industry and transportation(Wang et al., 2013). Guangzhou is the core megacity
81 in South subtropical region of China, where the atmospheric environment is complex and the
82 atmospheric oxidation level is high(Tan et al., 2019). The high emissions of inorganic nitrogen
83 form anthropogenic combustion sources have serious and profound impacts on the
84 environment. In this study, we aimed to comprehensive clarify the level of inorganic Nr and
85 revisit the source layout of atmospheric inorganic Nr .



86 2. Experimental and theoretical methods

87 2.1. Sampling and Chemical concentration analysis

88 PM_{2.5} samples (n=66) were collected from May 2017 to June 2018 in Guangzhou
89 (23.13°N, 113.27°E). Details of sample collection can be found in our previous study(Jiang et
90 al., 2021a). The chemical components including water-soluble ions (i.e., NH₄⁺, K⁺, Na⁺, Ca²⁺,
91 Mg²⁺, Cl⁻, NO₃⁻, and SO₄²⁻), organic carbon (OC), element carbon (EC), and organic molecular
92 markers (e.g., levoglucosan) were analyzed in our previous studies (SI Text S1)(Jiang et al.,
93 2021a; Jiang et al., 2021b). Moreover, meteorological parameters (temperature, relative
94 humidity (RH), atmosphere pressure, and wind speed) and the concentration of trace gases (CO,
95 SO₂, NO, NO₂, and O₃) were acquired by online instruments (details shown in SI Text S1). A
96 circular punch (r=1cm) of the sample filter was wrapped in a tin boat and then measured in an
97 elemental analyzer to determine the concentrations of TN.

98 2.2. Isotope analysis

99 The δ¹⁵N-NO₃⁻ and δ¹⁸O-NO₃⁻ values in PM_{2.5} was analyzed by methods of nitrous oxide
100 (N₂O), which was described in previous study in detail(Zong et al., 2017). Briefly, NO₃⁻ was
101 reduced to NO₂⁻ using cadmium powder and imidazole solution, and N₂O was made by adding
102 NaN₃ to NO₂⁻ solution. The production of 75nmol N₂O gas was needed to measure. The N₂O
103 gas produced by above processes was measured by MAT253 stable isotope mass spectrometer.
104 The values of δ¹⁸O and δ¹⁵N were expressed in per mil (‰) shown in Eq. (1) and (2), relative
105 to the international oxygen and nitrogen isotope standard, respectively.

$$106 \quad \delta^{15}N = \left[\frac{(^{15}N/^{14}N)_{sample}}{(^{15}N/^{14}N)_{standard}} - 1 \right] * 1000 \quad (1)$$

$$107 \quad \delta^{18}O = \left[\frac{(^{18}O/^{16}O)_{sample}}{(^{18}O/^{16}O)_{standard}} - 1 \right] * 1000 \quad (2)$$

108 The δ¹⁵N-NH₄⁺ was measured by methods of hypobromite oxidation coupled with
109 reduction of hydroxylamine hydrochloride(Sun et al., 2021). Briefly, NH₄⁺ was oxidated to
110 NO₂⁻ using alkaline hypobromite (BrO⁻), and N₂O was made by adding sodium arsenite and
111 hydrochloric acid to NO₂⁻ solution. The production of 120 nmol N₂O gas was needed to
112 measure. The N₂O gas produced by above processes was measured by MAT253 stable isotope
113 mass spectrometer. The values of δ¹⁵N were expressed in per mil (‰), Eq. (1). ⁷Be and ²¹⁰Pb



114 were acquired and details shown in [SI Text S1](#).

115 **2.3. Bayesian mixing and IsoSource model**

116 $\delta^{15}\text{N}$ were used for tracing source based on conservation of isotopic mass. Bayesian
117 mixing model improved upon linear mixing models by explicitly considering uncertainty in
118 prior information and isotopic equilibrium fractionation. Recently, Bayesian mixing model was
119 applied to trace the sources of atmospheric pollutants (Zong et al., 2017; Zong et al., 2020). The
120 model coupled with $\delta^{15}\text{N-NO}_3^-$ and $\delta^{18}\text{O-NO}_3^-$ were used to identify formation process and
121 quantify the sources contribution of NO_3^- (details presented in [SI Text S2](#)).

122 IsoSource model was released by Environmental Protection Agency (EPA), could
123 calculate ranges of source contributions to a mixture based on conservation of isotopic mass
124 when number of sources is too large to permit a unique solution and provide the distribution of
125 source proportions (Phillips et al., 2005). IsoSource model coupled with $\delta^{15}\text{N-NH}_4^+$ were
126 applied to quantify the NH_4^+ source (details presented in [SI Text S2](#)).

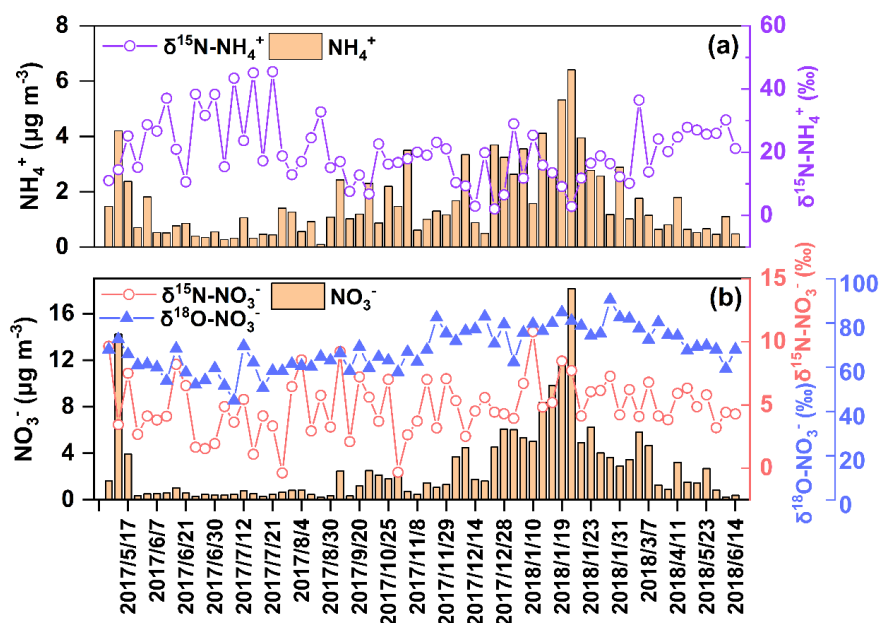
127 **3. Results and discussion**

128 **3.1. Concentration and seasonal variation of NH_4^+ and NO_3^-**

129 The concentration of NH_4^+ and NO_3^- in $\text{PM}_{2.5}$ was $1.6\pm 1.3 \mu\text{g m}^{-3}$ and $2.8\pm 3.4 \mu\text{g m}^{-3}$,
130 contributed 18.7% and 32.6% to SIA. The concentration of N-NH_4^+ and N-NO_3^- was 1.2 ± 1.0
131 $\mu\text{g m}^{-3}$ and $0.6\pm 0.8 \mu\text{g m}^{-3}$, contributed 45.8% and 23.2% to TN, respectively; thus, NH_4^+ and
132 NO_3^- were essential part of nitrogen aerosols. NH_4^+ and NO_3^- showed similar seasonal
133 variations with higher concentrations in winter than in summer ([Fig. 1](#)). During winter the air
134 mass was often dry and cold with low wind speed, which meant the decrease of the atmospheric
135 self-purification capability. In addition, primary combustion source related to fossil fuel and
136 biomass burning always showed significant increase in North China in winter, which greatly
137 increased the concentration of atmospheric pollutants in Guangzhou by long-range
138 transportation. However, during summer, the air mass from sea was relatively clean with high
139 wind speed facilitating the diffusion of pollutants. Moreover, high temperature in summer was
140 conducive to the decomposition of NH_4NO_3 (Song et al., 2008). Thus, the levels of NH_4^+ and



141 NO_3^- were lower in summer. In addition, concentrations of NH_4^+ and NO_3^- in our study, were
142 lower than North China [Beijing(Wu et al., 2019; Fan et al., 2022), Tianjin(Xiang et al., 2022),
143 Shijiazhuang(Xiang et al., 2022), and Harbin(Sun et al., 2021)], East China [Nanchang(Xiao
144 et al., 2020)], and Central China [Wuhan and Changsha(Xiao et al., 2020; Zong et al., 2020)],
145 suggested the level of air pollution in Guangzhou has been alleviated to a certain extent.
146 Therefore, it is necessary to conduct comprehensive study on the emission sources of NH_4^+ and
147 NO_3^- to take more effective measures to mitigate air pollution.



148

149 **Figure 1.** The concentration and $\delta^{15}\text{N}$ of NH_4^+ (a) and concentration, $\delta^{15}\text{N}$, and $\delta^{18}\text{O}$ of NO_3^-
150 (b).

151 3.2. Characteristic and seasonal variation in $\delta^{15}\text{N-NH}_4^+$ and source apportionment of 152 NH_4^+

153 The $\delta^{15}\text{N-NH}_4^+$ values over Guangzhou ranged from 2.1‰ to 45.5‰, with an annual mean
154 of $20.2 \pm 10.1\%$. In our study, the $\delta^{15}\text{N-NH}_4^+$ values were comparable to those at suburban sites
155 (Fig. S1) such as sites in Japan ($22.1 \pm 8.3\%$, $16.1 \pm 6.6\%$)(Kawashima and Kurahashi, 2011)
156 and Korea (Jeju Island, $17.4 \pm 4.9\%$)(Kundu et al., 2010) but heavier than those in polluted
157 regions, such as Heshan in Pearl River Delta (PRD) (average $+7.17\%$)(Liu et al., 2018) and
158 Beijing (-37.1% to $+5.8\%$)(Pan et al., 2016). $\delta^{15}\text{N-NH}_4^+$ values were lower in autumn (17.3‰)



159 and winter (14.4‰) than in spring (22.5‰) and summer (25.7‰), which was similar to the
160 trends in Japan (Kawashima and Kurahashi, 2011).

161 The seasonal differences in $\delta^{15}\text{N-NH}_4^+$ values were significant between warm
162 (summer/spring) and cool seasons (winter/fall) ($p < 0.05$). The $\delta^{15}\text{N-NH}_4^+$ was affected by the
163 ratio of $\text{NH}_4^+(\text{NH}_3+\text{NH}_4^+)$ (Text S3). A linear fitting equation was observed between
164 $\text{NH}_4^+(\text{NH}_3+\text{NH}_4^+)$ and $\delta^{15}\text{N-NH}_4^+$, and the absolute value of the slope (32.4) approximated the
165 isotope equilibrium fractionation value (+33%) between atmospheric NH_3 and NH_4^+ (Fig. S2).
166 The linear fitting suggested that the lower the NH_4^+ proportion was, the heavier the $\delta^{15}\text{N-NH}_4^+$
167 value. The lower NH_4^+ level was accordance with higher $\delta^{15}\text{N-NH}_4^+$ in summer, which was the
168 opposite of winter. In addition, previous study suggested that the marked variation in $\delta^{15}\text{N-NH}_4^+$
169 NH_4^+ values was largely controlled by the emission sources of NH_3 , the precursor gas of
170 NH_4^+ (Liu et al., 2018). According to the $\delta^{15}\text{N-NH}_4^+$ results, the source of NH_4^+ was assigned
171 as biomass burning (27.9±16.4%), coal combustion (16.0±3.9%), vehicles (19.8±5.3%),
172 fertilizer (10.9±6.1%), livestock (12.7±5.8%), and urban waste (11.9±6.1%), shown in Fig. 2a.

173 In our study, non-agriculture sources were the dominators of NH_4^+ (75.1%). Unexpectedly,
174 the contribution of biomass burning was the highest. Especially, from late June to July, the
175 contribution of biomass burning enhanced, which possibly resulted from sugarcane leaf
176 burning. The $\delta^{15}\text{N}$ in sugarcane leaf was as high as 38‰ (Martinellia et al., 2002). The $\delta^{15}\text{N-NH}_4^+$
177 NH_4^+ released from sugarcane leaf was estimated as 44.1‰ (SI Text S4), which coincided with
178 the highest $\delta^{15}\text{N-NH}_4^+$ value in July (45.5‰ and 45.1‰). In PRD, south winds prevail in July
179 and the sampling site is located downwind of sugarcane planting area. Therefore, the air mass
180 to sampling site might carry the pollutants related to sugarcane leaf burning. K^+ is a typical
181 biomass burning tracer (Cui et al., 2018). Considering the impact of primary emission intensity,
182 $[\text{NH}_4^+/\text{EC}]$ and $[\text{K}^+/\text{EC}]$ were used to calculate the correlation coefficient ($r=0.435$, $p < 0.01$),
183 which verified NH_4^+ was influenced by biomass burning. In recent years, biomass burning has
184 been gradually identified as an important source of NH_4^+ (Meng et al., 2017; Xiao et al., 2020).
185 The results based on emission inventories showed that the contribution of residential biomass
186 combustion to NH_3 ranged from 33% to 53% in China (Meng et al., 2017). According to $\delta^{15}\text{N}$,
187 biomass burning contributed 18% [Harbin, East North China] (Sun et al., 2021), 46% [Wuhan,
188 South Central China], 40% [Changsha, South Central China] (Xiao et al., 2020), 35%



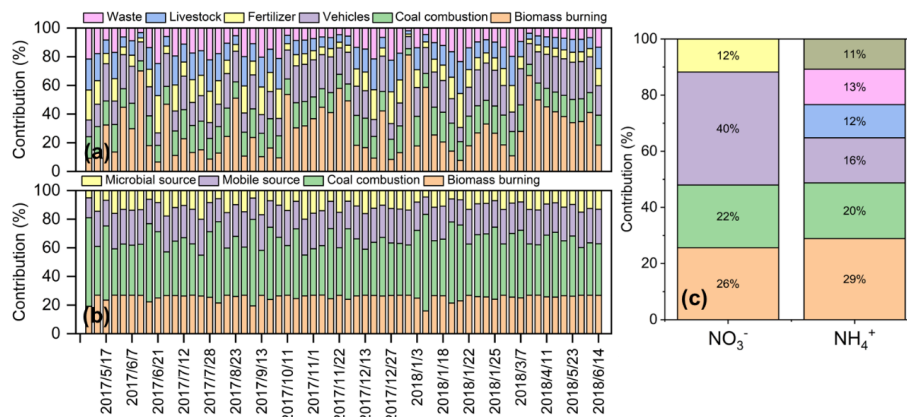
189 [Nanchang, East China](Xiao et al., 2020), and 23% [Guangzhou, South China](Chen et al.,
190 2022) to NH_4^+ . Particularly, in Guangzhou the contribution of biomass burning in ground was
191 higher than that in Guangzhou tower with the height of 488 meters, suggested that the influence
192 of regional biomass burning(Chen et al., 2022). Furthermore, ^7Be is mainly originated from
193 upper atmosphere, whereas ^{210}Pb is derived from terrestrial surface(Jiang et al., 2021b). High
194 level of ^7Be observed in ground suggested the sink influence of upper atmosphere. ^7Be and
195 ^{210}Pb are chemically stable and with unique sources, which can effectively reflect the transport
196 of continental air mass and the air exchange between stratosphere and troposphere. In our study,
197 the correlation coefficient between NH_4^+ and ^{210}Pb ($r=0.701$, $p < 0.01$) was higher than that
198 between NH_4^+ and ^7Be ($r=0.432$, $p < 0.01$), suggested that NH_4^+ was mainly affected by
199 regional emission. Therefore, biomass burning exerted essential influence on NH_4^+ level, which
200 should no longer be ignored.

201 In addition, with the acceleration of urbanization, combustion sources related to fossil
202 fuels have become the main sources of NH_3 . In previous studies, source of NH_x ($\text{NH}_3+\text{NH}_4^+$)
203 was mainly from agriculture activity due to rough way of farming(Chang et al., 2016; Pan et
204 al., 2020). However, with the improvement of efficient fertilization practices, agricultural NH_3
205 decreased significantly(Wang et al., 2022). Fossil fuels, such as coal and gasoline, are major
206 energies for production and domestic using, and their contribution to NH_3 has become
207 increasingly important. In North China, fossil fuel combustion contributed 92% to NH_3 during
208 hazes(Zhang et al., 2020; Pan et al., 2016). In previous study of Guangzhou, the contribution
209 of NH_3 from fossil source in ground observations (43%) was higher than the observed in
210 Guangzhou tower (18%), indicated the importance of locally related fossil fuel combustion
211 source(Chen et al., 2022). In our study, vehicle emission and coal combustion contributed
212 $19.8\pm 5.3\%$ and $16.0\pm 3.9\%$ of NH_4^+ respectively, which was lower than the North China but
213 higher than agricultural sources. The share of NH_3 from vehicle exhaust was estimated to be
214 18.8% based on the emission factor of NH_3 from on road vehicles in Guangzhou, which was
215 similar to our results(Liu et al., 2014). The selective catalytic reduction process for vehicle can
216 reduce NO_x , but increased emission of NH_3 , which has confirmed as an important source of
217 NH_3 (Heeb et al., 2006; Meng et al., 2017). Despite the efforts of government to promote
218 electric vehicles in recent years, their share is still relatively low (about 5%). As increasing car



219 ownership, this has an important impact on atmospheric NH_3 . Coal combustion was the second
220 most important source of fossil combustion after vehicle emissions in our study, although the
221 contribution was lower than in North China(Wu et al., 2019; Zhang et al., 2020; Pan et al.,
222 2016). The absence of heating in Guangzhou may explain the lower contribution of coal
223 combustion compared to the North. On an annual basis, the contribution of fossil fuel-related
224 combustion sources in our study (35.8%) was comparable to that in North China (37%-
225 52%)(Pan et al., 2018).

226 The source contributions of NH_4^+ in our study were compared to other regions, shown in
227 **Fig. S3**. The combustion related sources (biomass burning, coal combustion, and vehicle) have
228 gradually become the dominant source of urban atmospheric NH_3 . Biomass burning and
229 vehicle could emit massive carbon monoxide (CO)(Li and Wang, 2007; Wang et al., 2005). In
230 Guangzhou, NH_4^+ was positively related to CO ($r=0.637$, $p < 0.01$), which confirmed
231 combustion sources playing a key role in NH_4^+ . From a historical perspective, NH_3 emissions
232 from anthropogenic combustion and industry have been steadily increasing since 1960(Meng
233 et al., 2017). The optimization of energy structure and encouragement of development new
234 energy vehicle would be hopeful to reduce NH_3 . The results of this study would be conducive
235 to reduce NH_3 scientifically and effectively, and would relieve the pressure on the reduction
236 from agricultural source.



237
238 **Figure 2.** The sources apportionment results of atmospheric NH_4^+ (a) and NO_3^- (b) in
239 Guangzhou, and the comparison of sources results between NH_4^+ and NO_3^- (c).



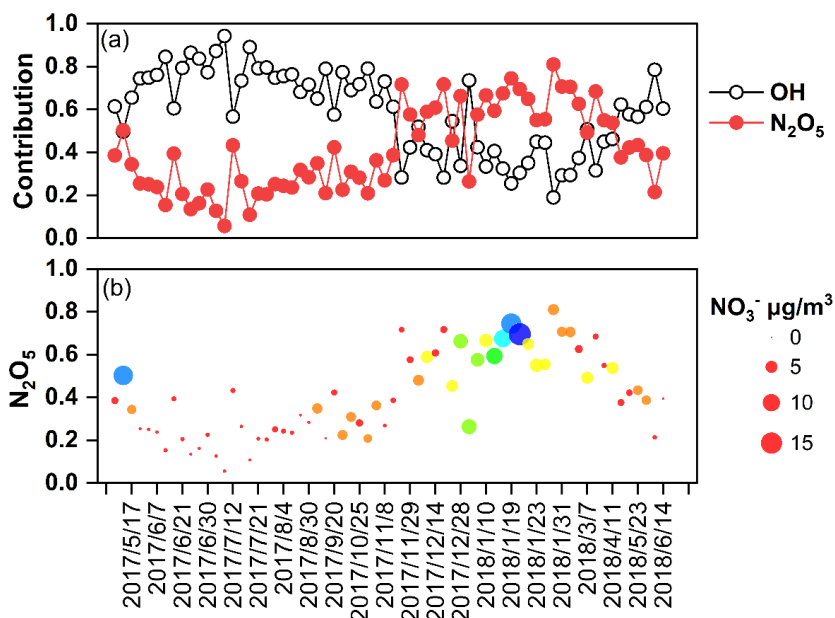
240 **3.3. Characteristic and seasonal variation in $\delta^{18}\text{O}\text{-NO}_3^-$ and $\delta^{15}\text{N}\text{-NO}_3^-$ and source**
241 **apportionment of NO_3^-**

242 **3.3.1. Seasonal variation of $\delta^{18}\text{O}\text{-NO}_3^-$**

243 The $\delta^{18}\text{O}\text{-NO}_3^-$ in Guangzhou was $68.1\pm 9.7\text{‰}$ (44.9‰ to 90.5‰) comparable to that in
244 precipitation ($66.3\pm 2.8\text{‰}$)(Fang et al., 2011), but lower than those regions with weak light
245 intensity, such as BeiChengHuang Island ($76.6\pm 8.1\text{‰}$)(Zong et al., 2017) and Bermuda Islands
246 ($71.1\pm 3.0\text{‰}$)(Hastings et al., 2003). In this study, $\delta^{18}\text{O}\text{-NO}_3^-$ was higher in winter and spring
247 than in summer and autumn, which was similar to the seasonal variation in $\delta^{18}\text{O}\text{-NO}_3^-$ in
248 previous studies (Fang et al., 2011; Gobel et al., 2013). On the one hand, $\delta^{18}\text{O}\text{-NO}_3^-$ value was
249 associated with formation pathways of NO_3^- . The results simulated by Bayesian mixing model
250 suggested that the contributions of N_2O_5 channel to NO_3^- were 56.8%, 58.9%, 29.2%, and 27.0%
251 in winter, spring, fall, and summer, respectively. The $\delta^{18}\text{O}$ value of NO_3^- formed by N_2O_5
252 channel is higher than that by $\cdot\text{OH}$ pathway (SI Text S5). The night in cold season was longer
253 than that in warm season, which favored NO_3^- formation through N_2O_5 channel. In addition,
254 the illumination intensity was weakened in cold season compared with that in warm season,
255 which constrained the production of $\cdot\text{OH}$ (Zong et al., 2020; Tan et al., 2019; Wang et al., 2017).
256 Thus, the contribution of the N_2O_5 channel in cold season was higher than that in warm season.
257 Furthermore, concentration of NO_3^- was high when contribution of N_2O_5 channel enhanced
258 (Fig. 3), suggested NO_3^- pollution was related to N_2O_5 hydrolysis pathway. The air mass to
259 Guangzhou was derived from the South China Sea in summer and the North continental region
260 in winter. The higher $\delta^{18}\text{O}\text{-NO}_3^-$ and NO_3^- concentration might be affected by long-range and
261 high-altitude transport from North China, which might carry abundant of precursors. Massive
262 NO_3^- could formed by N_2O_5 hydrolysis at high altitude and transported to the ground. The index
263 of $f(^7\text{Be}, ^{210}\text{Pb})$ was expressed in SI Text S1 and could reflect the influence of atmospheric
264 dynamic transport on aerosol pollutants(Jiang et al., 2021b). Generally, air masses with low
265 values of $f(^7\text{Be}, ^{210}\text{Pb})$ suggested that pollutants were associated with continental surface
266 emission, whereas high $f(^7\text{Be}, ^{210}\text{Pb})$ were influenced by long-range transport from upper air
267 masses. The contribution of N_2O_5 channel was positively correlated with $f(^7\text{Be}, ^{210}\text{Pb})$ ($r=0.319$,
268 $p < 0.05$), indicated the long-range transport influence of upper air mass on N_2O_5 channel. For
269 example, on 25 January 2018, the contribution of N_2O_5 channel (nitrate) was 81.1% ($3.6 \mu\text{g m}^{-3}$



270 ³), when the upper air mass was from the North China. However, on 7 July 2017, the N₂O₅
271 channel (nitrate) contributed only 5.7% (0.5 μg m⁻³) corresponding to the air mass mainly from
272 the South China Sea transported at low-altitude (Fig. S4).



273
274 **Figure 3.** The contribution of the OH radical oxidation and N₂O₅ hydrolysis pathway to NO₃⁻
275 (a). The vertical position of dots corresponded to the contribution of N₂O₅ pathway and the size
276 of the dots corresponded to the concentration of NO₃⁻ (b).

277 $\delta^{18}\text{O}-\text{NO}_3^-$ decreased from 76.7‰ in 2014 to 68.1‰ in 2017-2018 (Zong et al., 2020),
278 which indicated that $\cdot\text{OH}$ channel became more important in Guangzhou. The enhanced
279 contribution of $\cdot\text{OH}$ pathway indicated the increasing atmospheric oxidation capacity. In recent
280 years, although the concentration of PM_{2.5} in Guangzhou has significantly decreased, the
281 photochemical pollution caused by high O₃ concentrations was not optimistic (Tan et al., 2019).
282 The O₃ concentration in the PRD showed a fluctuating upward trend from 2013 to 2020;
283 especially in 2017-2018 O₃ concentrations were at high levels (Environmental Status Bulletin
284 of Guangdong Province Fig. S5). In our study, the NO₃⁻ formation pathway inferred from $\delta^{18}\text{O}-$
285 NO₃⁻ proved the enhancement of atmospheric oxidation capacity.



286 3.3.2. Seasonal variation of $\delta^{15}\text{N-NO}_3^-$ and source apportionment of NO_3^-

287 **Seasonal variation of $\delta^{15}\text{N-NO}_3^-$.** The $\delta^{15}\text{N-NO}_3^-$ in Guangzhou was $4.9\pm 2.2\text{‰}$ (-0.4‰
288 to 10.8‰), which was similar to the wet deposition (Fang et al., 2011). The $\delta^{15}\text{N-NO}_3^-$ was
289 comparable to that from the Northeast United States (6.8‰) (Elliott et al., 2009), and lower
290 than regions in China, where NO_3^- was predominantly derived from anthropogenic sources,
291 such as Heshan in Guangdong ($7.50\pm 3.30\text{‰}$) (Su et al., 2020), BeiChengHuang Island
292 ($8.20\pm 6.20\text{‰}$) (Zong et al., 2017), and Beijing ($12.1\pm 3.3\text{‰}$) (Fan et al., 2022). Nevertheless, the
293 $\delta^{15}\text{N-NO}_3^-$ in this study was significantly higher than those from clean background regions,
294 where NO_3^- was mainly from natural sources, such as the coast of Antarctica ($-$
295 $12.4\pm 7.20\text{‰}$) (Savarino et al., 2007) and Bermuda ($-2.1\pm 1.5\text{‰}$ warm season, $-5.9\pm 3.3\text{‰}$ cool
296 season) (Hastings et al., 2003). The values of $\delta^{15}\text{N-NO}_3^-$ in winter, spring, summer, and autumn
297 were 5.6‰ , 5.3‰ , 4.4‰ , and 4.5‰ , respectively. The $\delta^{15}\text{N-NO}_3^-$ in winter and summer
298 showed significant difference ($p < 0.05$). The values of $\delta^{15}\text{N-NO}_3^-$ were influenced by
299 atmospheric processes and emission sources (Elliott et al., 2009). For N_2O_5 channel, NO_3^- is
300 characterized by higher $\delta^{15}\text{N}$ values (Freyer et al., 1993; Elliott et al., 2009). The N_2O_5 channel
301 was the predominant formation pathway of NO_3^- in winter, which was in accordance with the
302 seasonal variation in $\delta^{15}\text{N-NO}_3^-$. In addition, the difference in $\delta^{15}\text{N-NO}_3^-$ reflected the variation
303 in the emission source of NO_3^- . $\delta^{15}\text{N-NO}_x$ from coal combustion was relatively high. In winter,
304 the higher $\delta^{15}\text{N-NO}_3^-$ probably related to long-range transport from North, where coal
305 combustion enhanced in winter.

306 **Source apportionment of NO_3^- .** Based on the Bayesian mixing model coupled with $\delta^{15}\text{N-}$
307 NO_3^- , NO_3^- sources were assigned as coal combustion $40.4\pm 8.7\%$, biomass burning $25.6\pm 2.1\%$,
308 mobile sources (vehicles) $22.3\pm 3.1\%$, and microbial process $11.7\pm 3.8\%$. **Figure 2b** and **Figure**
309 **S6** showed the source contribution of NO_3^- in Guangzhou and other regions in China,
310 respectively. Compared to earlier periods (2013-2014), concentration of NO_3^- from vehicle and
311 coal combustion decreased significantly (Zong et al., 2020), which resulted from the stricter
312 vehicle emission standard, promotion of new energy electric vehicles, and ultraclean
313 transformation of coal combustion. However, almost all production and domestic segments
314 rely on energy generated from coal combustion, which was still dominant source of NO_3^- in



315 2017-2018. Coal combustion was affected not only by local emissions but also by external air
316 mass transmission. The contribution of coal combustion was higher in winter than in summer,
317 which probably related to the long-range transportation from North. Taking 10 January 2018
318 as an example, the contribution of coal combustion sources to NO_3^- was 67.5%, and the
319 corresponding air mass was from the North and transmitted to Guangzhou through high altitude.
320 However, the air mass on 26 July 2017 were mainly from the South China Sea, which was
321 transmitted through low-altitude to Guangzhou. The contribution of coal burning to NO_3^- on
322 26 July 2017 was 28.5% lower than that on 10 January 2018.

323 As non-fossil combustion source, biomass burning was also an important source of NO_3^-
324 and accounted for 25.6%. The contribution of biomass burning and vehicle was stable through
325 a year. Another non-fossil source is related to soil microbial activity and only contributed 11.7%
326 to NO_3^- , which unexpectedly lower than the results in earlier periods (2013-2014). Generally,
327 the microorganisms in soil emit NO through nitrification or denitrification, which was affected
328 by the amount of carbon and nitrogen nutrients in soil (Hall and Matson, 1996). In earlier
329 periods, due to the higher level of aerosols, the amount of nutrients settling in soil was also
330 higher, which was exemplified by the observation of dry and wet deposition in Guangzhou (He
331 et al., 2022; Zheng et al., 2020). In addition, the reduction of cultivated land from 2013 to 2018
332 might also reduce the contribution of microbial source emissions. Therefore, emissions from
333 natural sources were also influenced by human activities to some extent. The contribution of
334 microbial process was higher in summer than in winter. In summer, higher RH and temperature
335 were favorable for intense activity of soil microorganisms (Zong et al., 2017). The contributions
336 of microbial processes to NO_3^- also decreased in winter compared with summer at regional
337 background sites and five Chinese megacities, including Guangzhou (Zong et al., 2017; Zong
338 et al., 2020).

339 The sources comparison between NO_3^- and NH_4^+ was shown in Fig. 2c. Coal combustion,
340 biomass burning, and vehicles were three significant sources of NO_3^- and NH_4^+ . Coal
341 combustion and biomass burning were the dominant sources of NO_3^- and NH_4^+ , respectively.
342 The vehicles were also important source of atmospheric inorganic N_r contributed to 22.3% and
343 19.8% to NO_3^- and NH_4^+ , respectively. Recently, the government has actively taken many
344 measures to reduce the pollution from vehicles, such as stricter automobile emission standards



345 and the promotion of new energy vehicles. However, due to the large vehicle ownership base,
346 the pollutants emitted from vehicles are not optimistic. In addition, vehicles emissions could
347 contribute half of the fresh secondary organic aerosol in urban environment(Zhang et al., 2022;
348 Zhao et al., 2022a).

349 **4. Conclusions**

350 A year-long field observation was conducted in Guangzhou to clarify the atmospheric fate
351 of inorganic nitrogen aerosol. Inorganic nitrogen species were the most essential component of
352 TN including NH_4^+ (45.8%) and NO_3^- (23.2%), which are also dominant components of SIA
353 and play a key role in China haze. The $\delta^{15}\text{N}$ is a powerful tool to quantify the source
354 contribution of NH_4^+ and NO_3^- , which suggested that anthropogenic combustion sources (coal
355 combustion, biomass burning, and vehicles) were the dominant sources.

356 Anthropogenic combustion sources contributed 63.2% to NH_4^+ higher than agricultural
357 sources (23.6%). NH_3 largely facilitates the formation of sulfate and nitrate. Meanwhile, sulfate
358 and nitrate promote each other with positive feedback effect, which could trigger haze. In
359 megacities of China, the focus of NH_3 reduction should be on anthropogenic combustion
360 sources especially on biomass burning, which might be responsible for the lag of the decline
361 in deposition of air pollutions behind the reduction in emission(Zhao et al., 2022b). In addition,
362 anthropogenic combustion sources accounted for 88.3% of NO_3^- . Coal combustion and
363 vehicles contributed 40.4% and 22.3% to NO_3^- , respectively. Despite a series of measures to
364 reduce emissions of NO_x , fossil fuels, as the main energy for production and living, will still
365 inevitably emit a large amount of NO_x . Our results emphasized that the emission of
366 atmospheric inorganic nitrogen is largely related to anthropogenic combustion sources. The
367 development and promotion of clean energy and efficient use of biomass are conducive to the
368 deep reduction of atmospheric nitrogen.

369 **Data availability**

370 The original data of this research (stable nitrogen isotopes and inorganic nitrogen
371 concentrations) are available at Mendeley data (Li and Li, 2023). The Iso Source model was



372 download from Environmental Protection Agency, via their website:
373 https://www.epa.gov/sites/default/files/2015-11/isosourcev1_3_1.zip.

374 **Author contributions**

375 Funding acquisition: Jun Li
376 Investigation: Tingting Li, Zeyu Sun, and Hongxing Jiang
377 Methodology: Tingting Li, Zeyu Sun, Hongxing Jiang, Jun Li, and Chongguo Tian
378 Project Administration: Jun Li
379 Resources: Jun Li, Chongguo Tian and Gan Zhang
380 Software: Tingting Li
381 Validation: Tingting Li and Jun Li
382 Writing – original draft: Tingting Li
383 Writing – review & editing: Jun Li

384 **Competing interests**

385 The authors declare that they have no conflict of interest.

386 **Financial support**

387 This study was supported by the Natural Science Foundation of China (NSFC; Nos.
388 (41977177), Guangdong Basic and Applied Basic Research Foundation (2021A1515011456),
389 Guangdong Foundation for Program of Science and Technology Research (Grant No.
390 2019B121205006 and 2020B1212060053).

391 **References**

392 Bhattarai, H., Zhang, Y. L., Pavuluri, C. M., Wan, X., Wu, G., Li, P., Cao, F., Zhang, W., Wang, Y., Kang, S., Ram,
393 K., Kawamura, K., Ji, Z., Widory, D., and Cong, Z.: Nitrogen speciation and isotopic composition of aerosols
394 collected at Himalayan Forest (3326 m a.s.l.): seasonality, sources, and implications, *Environ. Sci. Technol.*,
395 53, 12247–12256, <https://doi.org/10.1021/acs.est.9b03999>, 2019.
396 Breemen, N. V.: Nitrogen cycle natural organic tendency, *Nature*, 415, <https://doi.org/10.1038/415381a>, 2002.
397 Chang, Y., Liu, X., Deng, C., Dore, A. J., and Zhuang, G.: Source apportionment of atmospheric ammonia before,
398 during, and after the 2014 APEC summit in Beijing using stable nitrogen isotope signatures, *Atmos. Chem.*



- 399 Phys., 16, 11635-11647, <https://doi.org/10.5194/acp-16-11635-2016>, 2016.
- 400 Chen, Z., Pei, C., Liu, J., Zhang, X., Ding, P., Dang, L., Zong, Z., Jiang, F., Wu, L., Sun, X., Zhou, S., Zhang, Y.,
401 Zhang, Z., Zheng, J., Tian, C., Li, J., and Zhang, G.: Non-agricultural source dominates the ammonium aerosol
402 in the largest city of South China based on the vertical $\delta^{15}\text{N}$ measurements, *Sci. Total Environ.*, 848, 157750,
403 <https://doi.org/10.1016/j.scitotenv.2022.157750>, 2022.
- 404 Cui, M., Chen, Y., Zheng, M., Li, J., Tang, J., Han, Y., Song, D., Yan, C., Zhang, F., Tian, C., and Zhang, G.:
405 Emissions and characteristics of particulate matter from rainforest burning in the Southeast Asia, *Atmos.*
406 *Environ.*, 191, 194-204, <https://doi.org/10.1016/j.atmosenv.2018.07.062>, 2018.
- 407 Dunne, E. M., Gordon, H., Kürten, A., Almeida, J., Duplissy, J., Williamson, C., Ortega, I. K., Pringle, K. J.,
408 Adamov, A., and Schobesberger, S.: Global atmospheric particle formation from cern cloud measurements,
409 *Science*, 354, 1119-1123, <https://doi.org/10.1126/science.aaf2649>, 2016.
- 410 Elliott, E. M., Kendall, C., Wankel, S. D., Burns, D. A., Boyer, E. W., Harlin, K., Bain, D. J., and Butler, T. J.:
411 Nitrogen isotopes as indicators of NO_x source contributions to atmospheric nitrate deposition across the
412 midwestern and Northeastern United States, *Environ. Sci. Technol.*, 41, 7661-7667,
413 <https://doi.org/10.1021/es070898t>, 2007.
- 414 Elliott, E. M., Kendall, C., Boyer, E. W., Burns, D. A., Lear, G. G., Golden, H. E., Harlin, K., Bytnerowicz, A.,
415 Butler, T. J., and Glatz, R.: Dual nitrate isotopes in dry deposition: Utility for partitioning NO_x source
416 contributions to landscape nitrogen deposition, *J. Geophys. Res.*, 114, <https://doi.org/10.1029/2008JG000889>,
417 2009.
- 418 Fan, M.-Y., Zhang, Y.-L., Hong, Y., Lin, Y.-C., Zhao, Z.-Y., Cao, F., Sun, Y., Guo, H., and Fu, P.: Vertical
419 differences of nitrate sources in urban boundary layer based on tower measurements, *Environ. Sci. Technol.*
420 *Lett.*, 2c00600, <https://doi.org/10.1021/acs.estlett.2c00600>, 2022.
- 421 Fang, Y. T., Koba, K., Wang, X. M., Wen, D. Z., Li, J., Takebayashi, Y., Liu, X. Y., and Yoh, M.: Anthropogenic
422 imprints on nitrogen and oxygen isotopic composition of precipitation nitrate in a nitrogen-polluted city in
423 southern China, *Atmos. Chem. Phys.*, 11, 1313-1325, <https://doi.org/10.5194/acp-11-1313-2011>, 2011.
- 424 Freyer, H. D., Kley, D., Volz-Thomas, A., and Kobel, K.: On the interaction of isotopic exchange processes with
425 photochemical reactions in atmospheric oxides of nitrogen, *J. Geophys. Res.*, 98, 14,791-714,796,
426 <https://doi.org/10.1029/93JD00874>, 1993.
- 427 Fu, X., Wang, S., Xing, J., Zhang, X., Wang, T., and Hao, J.: Increasing ammonia concentrations reduce the
428 effectiveness of particle pollution control achieved via SO₂ and NO_x emissions reduction in East China, *Environ.*
429 *Sci. Technol. Lett.*, 4, 221-227, <https://doi.org/10.1021/acs.estlett.7b00143>, 2017.
- 430 Galloway, J. N., Dentener, F. J., Capone, D. G., Boyer, E. W., Howarth, R. W., Seitzinger, S. P., Asner, G. P.,
431 Cleveland, C. C., Green, P. A., Holland, E. A., Karl, D. M., Michaels, A. F., Porter, J. H., Townsend, A. R., and
432 VörO'smarty, C. J.: Nitrogen cycles past present and future, *Biogeochemistry*, 70, 153-226,
433 <https://doi.org/10.1007/s10533-004-0370-0>, 2004.
- 434 Gobel, A. R., Altieri, K. E., Peters, A. J., Hastings, M. G., and Sigman, D. M.: Insights into anthropogenic nitrogen
435 deposition to the North Atlantic investigated using the isotopic composition of aerosol and rainwater nitrate,
436 *Geophys. Res. Lett.*, 40, 5977-5982, <https://doi.org/10.1002/2013gl058167>, 2013.
- 437 Hall, S. J. and Matson, P. A.: NO_x emissions from soil: implications for air quality modeling in agricultural regions,
438 *Annu. Rev. Energy Environ.*, 21, 311-346, <https://doi.org/10.1146/annurev.energy.21.1.311>, 1996.
- 439 Hastings, M. G., Sigman, D. M., and Lipschultz, F.: Isotopic evidence for source changes of nitrate in rain at
440 Bermuda, *J. Geophys. Res.: Atmos.*, 108, 1-12, <https://doi.org/10.1029/2003jd003789>, 2003.
- 441 He, S., Huang, M., Zheng, L., Chang, M., Chen, W., Xie, Q., and Wang, X.: Seasonal variation of transport
442 pathways and potential source areas at high inorganic nitrogen wet deposition sites in southern China, *J. Environ.*



- 443 Sci. (China), 114, 444-453, <https://doi.org/10.1016/j.jes.2021.12.024>, 2022.
- 444 Heeb, N. V., Forss, A.-M., Brühlmann, S., Lüscher, R., Saxer, C. J., and Hug, P.: Three-way catalyst-induced
445 formation of ammonia—velocity- and acceleration-dependent emission factors, *Atmos. Environ.*, 40, 5986-
446 5997, <https://doi.org/10.1016/j.atmosenv.2005.12.035>, 2006.
- 447 Hodas, N., Sullivan, A. P., Skog, K., Keutsch, F. N., Collett, J. L., Jr., Decesari, S., Facchini, M. C., Carlton, A.
448 G., Laaksonen, A., and Turpin, B. J.: Aerosol liquid water driven by anthropogenic nitrate: implications for
449 lifetimes of water-soluble organic gases and potential for secondary organic aerosol formation, *Environ. Sci.*
450 *Technol.*, 48, 11127-11136, <https://doi.org/10.1021/es5025096>, 2014.
- 451 Holland, E. A., Dentener, F. J., Braswell, B. H., and Sulzman, J. M.: Contemporary and pre-industrial global
452 reactive nitrogen budgets, *Biogeochemistry*, 46, 7-43, <https://doi.org/10.1007/BF01007572>, 1999.
- 453 Huang, Z., Wang, S., Zheng, J., Yuan, Z., Ye, S., and Kang, D.: Modeling inorganic nitrogen deposition in
454 Guangdong province, China, *Atmos. Environ.*, 109, 147-160, <https://doi.org/10.1016/j.atmosenv.2015.03.014>,
455 2015.
- 456 Jiang, H., Li, J., Sun, R., Tian, C., Tang, J., Jiang, B., Liao, Y., Chen, C., and Zhang, G.: Molecular dynamics and
457 light absorption properties of atmospheric dissolved organic matter, *Environ. Sci. Technol.*, 55, 10268-10279,
458 <https://doi.org/10.1021/acs.est.1c01770>, 2021a.
- 459 Jiang, H., Li, J., Sun, R., Liu, G., Tian, C., Tang, J., Cheng, Z., Zhu, S., Zhong, G., Ding, X., and Zhang, G.:
460 Determining the sources and transport of brown carbon using radionuclide tracers and modeling, *J. Geophys.*
461 *Res.: Atmos.*, 126, e2021JD034616, <https://doi.org/10.1029/2021jd034616>, 2021b.
- 462 Kang, Y., Liu, M., Song, Y., Huang, X., Yao, H., Cai, X., Zhang, H., Kang, L., Liu, X., Yan, X., He, H., Zhang,
463 Q., Shao, M., and Zhu, T.: High-resolution ammonia emissions inventories in China from 1980 to 2012, *Atmos.*
464 *Chem. Phys.*, 16, 2043-2058, <https://doi.org/10.5194/acp-16-2043-2016>, 2016.
- 465 Kawashima, H. and Kurahashi, T.: Inorganic ion and nitrogen isotopic compositions of atmospheric aerosols at
466 Yurihonjo, Japan: implications for nitrogen sources, *Atmos. Environ.*, 45, 6309-6316,
467 <https://doi.org/10.1016/j.atmosenv.2011.08.057>, 2011.
- 468 Kundu, S., Kawamura, K., and Lee, M.: Seasonal variation of the concentrations of nitrogenous species and their
469 nitrogen isotopic ratios in aerosols at Gosan, Jeju Island: Implications for atmospheric processing and source
470 changes of aerosols, *J. Geophys. Res.*, 115, <https://doi.org/10.1029/2009jd013323>, 2010.
- 471 Li, T. and Li, J.: High contribution of anthropogenic combustion sources to atmospheric inorganic reactive
472 nitrogen in south China evidenced by isotopes, Mendeley data [data set],
473 <https://doi.org/10.17632/vck5xy22w2.1>, 2023.
- 474 Li, X. H. and Wang, S. X.: Particulate and trace gas emissions from open burning of wheat straw and corn stover
475 in China, *Environ. Sci. Technol.*, 41, 6052-6058, <https://doi.org/10.1021/es0705137>, 2007.
- 476 Liu, J., Ding, P., Zong, Z., Li, J., Tian, C., Chen, W., Chang, M., Salazar, G., Shen, C., Cheng, Z., Chen, Y., Wang,
477 X., Szidat, S., and Zhang, G.: Evidence of rural and suburban sources of urban haze formation in China: a case
478 study from the Pearl River Delta region, *J. Geophys. Res.: Atmos.*, 123, 4712-4726,
479 <https://doi.org/10.1029/2017jd027952>, 2018.
- 480 Liu, T., Wang, X., Wang, B., Ding, X., Deng, W., Lü, S., and Zhang, Y.: Emission factor of ammonia (NH₃) from
481 on-road vehicles in China: tunnel tests in urban Guangzhou, *Environ. Res. Lett.*, 9, 064027,
482 <https://doi.org/10.1088/1748-9326/9/6/064027>, 2014.
- 483 Liu, Y., Zhang, Y., Lian, C., Yan, C., Wang, Y., Ge, M., He, H., and Kulmala, M.: The promotion effect of nitrous
484 acid on aerosol formation in wintertime in Beijing: the possible contribution of traffic-related emissions, *Atmos.*
485 *Chem. Phys.*, 20, 13023-13040, <https://doi.org/10.5194/acp-20-13023-2020>, 2020.
- 486 Liu, Y., Feng, Z., Zheng, F., Bao, X., Liu, P., Ge, Y., Zhao, Y., Jiang, T., Liao, Y., Zhang, Y., Fan, X., Yan, C., Chu,



- 487 B., Wang, Y., Du, W., Cai, J., Bianchi, F., Petäjä, T., Mu, Y., He, H., and Kulmala, M.: Ammonium nitrate
488 promotes sulfate formation through uptake kinetic regime, *Atmos. Chem. Phys.*, 21, 13269–13286,
489 <https://doi.org/10.5194/acp-21-13269-2021>, 2021.
- 490 Martinellia, L. A., Camargoa, P. B., Laraa, L. B. L. S., Victoriaa, R. L., and Artaxo, P.: Stable carbon and nitrogen
491 isotopic composition of bulk aerosol particles in a C4 plant landscape of southeast Brazil, *Atmos. Environ.*, 36,
492 2427–2432, [https://doi.org/10.1016/S1352-2310\(01\)00454-X](https://doi.org/10.1016/S1352-2310(01)00454-X), 2002.
- 493 Meng, W., Zhong, Q., Yun, X., Zhu, X., Huang, T., Shen, H., Chen, Y., Chen, H., Zhou, F., Liu, J., Wang, X., Zeng,
494 E. Y., and Tao, S.: Improvement of a global high-resolution ammonia emission inventory for combustion and
495 industrial sources with new data from the residential and transportation sectors, *Environ. Sci. Technol.*, 51,
496 2821–2829, <https://doi.org/10.1021/acs.est.6b03694>, 2017.
- 497 Meng, Z., Xu, X., Lin, W., Ge, B., Xie, Y., Song, B., Jia, S., Zhang, R., Peng, W., Wang, Y., Cheng, H., Yang, W.,
498 and Zhao, H.: Role of ambient ammonia in particulate ammonium formation at a rural site in the North China
499 Plain, *Atmos. Chem. Phys.*, 18, 167–184, <https://doi.org/10.5194/acp-18-167-2018>, 2018.
- 500 Pan, Y., Tian, S., Liu, D., Fang, Y., Zhu, X., Gao, M., Gao, J., Michalski, G., and Wang, Y.: Isotopic evidence for
501 enhanced fossil fuel sources of aerosol ammonium in the urban atmosphere, *Environ. Pollut.*, 238, 942–947,
502 <https://doi.org/10.1016/j.envpol.2018.03.038>, 2018.
- 503 Pan, Y., Tian, S., Liu, D., Fang, Y., Zhu, X., Zhang, Q., Zheng, B., Michalski, G., and Wang, Y.: Fossil fuel
504 combustion-related emissions dominate atmospheric ammonia sources during severe haze episodes: evidence
505 from ¹⁵N-stable isotope in size-resolved aerosol ammonium, *Environ. Sci. Technol.*, 50, 8049–8056,
506 <https://doi.org/10.1021/acs.est.6b00634>, 2016.
- 507 Pan, Y., Gu, M., He, Y., Wu, D., Liu, C., Song, L., Tian, S., Lü, X., Sun, Y., Song, T., Walters, W. W., Liu, X.,
508 Martin, N. A., Zhang, Q., Fang, Y., Ferracci, V., and Wang, Y.: Revisiting the concentration observations and
509 source apportionment of atmospheric ammonia, *Adv. Atmos. Sci.*, 37, 933–938, <https://doi.org/10.1007/s00376-020-2111-2>, 2020.
- 511 Phillips, D. L., Newsome, S. D., and Gregg, J. W.: Combining sources in stable isotope mixing models: alternative
512 methods, *Oecologia*, 144, 520–527, <https://doi.org/10.1007/s00442-004-1816-8>, 2005.
- 513 Savarino, J., Kaiser, J., Morin, S., Sigman, D. M., and Thiemens, M. H.: Nitrogen and oxygen isotopic constraints
514 on the origin of atmospheric nitrate in coastal Antarctica, *Atmos. Chem. Phys.*, 7, 1925–1945,
515 <https://doi.org/10.5194/acp-7-1925-2007>, 2007.
- 516 Song, W., Liu, X. Y., Hu, C. C., Chen, G. Y., Liu, X. J., Walters, W. W., Michalski, G., and Liu, C. Q.: Important
517 contributions of non-fossil fuel nitrogen oxides emissions, *Nat. Commun.*, 12, 243,
518 <https://doi.org/10.1038/s41467-020-20356-0>, 2021.
- 519 Song, Y., Dai, W., Wang, X., Cui, M., Su, H., Xie, S., and Zhang, Y.: Identifying dominant sources of respirable
520 suspended particulates in Guangzhou, China, *Environ. Eng. Sci.*, 25, 959–968,
521 <https://doi.org/10.1089/ees.2007.0146>, 2008.
- 522 Su, T., Li, J., Tian, C., Zong, Z., Chen, D., and Zhang, G.: Source and formation of fine particulate nitrate in South
523 China: Constrained by isotopic modeling and online trace gas analysis, *Atmos. Environ.*, 231,
524 <https://doi.org/10.1016/j.atmosenv.2020.117563>, 2020.
- 525 Sun, X., Zong, Z., Li, Q., Shi, X., Wang, K., Lu, L., Li, B., Qi, H., and Tian, C.: Assessing the emission sources
526 and reduction potential of atmospheric ammonia at an urban site in Northeast China, *Environ. Res.*, 198, 111230,
527 <https://doi.org/10.1016/j.envres.2021.111230>, 2021.
- 528 Tan, Z., Lu, K., Jiang, M., Su, R., Wang, H., Lou, S., Fu, Q., Zhai, C., Tan, Q., Yue, D., Chen, D., Wang, Z., Xie,
529 S., Zeng, L., and Zhang, Y.: Daytime atmospheric oxidation capacity in four Chinese megacities during the
530 photochemically polluted season: a case study based on box model simulation, *Atmos. Chem. Phys.*, 19, 3493–



- 531 3513, <https://doi.org/10.5194/acp-19-3493-2019>, 2019.
- 532 Wang, C., Duan, J., Ren, C., Liu, H., Reis, S., Xu, J., and Gu, B.: Ammonia emissions from croplands decrease
533 with farm size in China, *Environ. Sci. Technol.*, 56, 9915-9923, <https://doi.org/10.1021/acs.est.2c01061>, 2022.
- 534 Wang, T., Xue, L., Brimblecombe, P., Lam, Y. F., Li, L., and Zhang, L.: Ozone pollution in China: a review of
535 concentrations, meteorological influences, chemical precursors, and effects, *Sci. Total Environ.*, 575, 1582-
536 1596, <https://doi.org/10.1016/j.scitotenv.2016.10.081>, 2017.
- 537 Wang, X., Carmichael, G., Chen, D., Tang, Y., and Wang, T.: Impacts of different emission sources on air quality
538 during March 2001 in the Pearl River Delta (PRD) region, *Atmos. Environ.*, 39, 5227-5241,
539 <https://doi.org/10.1016/j.atmosenv.2005.04.035>, 2005.
- 540 Wang, X., Wu, Z., Shao, M., Fang, Y., Zhang, L., Chen, F., Chan, P.-w., Fan, Q., Wang, Q., Zhu, S., and Bao, R.:
541 Atmospheric nitrogen deposition to forest and estuary environments in the Pearl River Delta region, southern
542 China, *Tellus B: Chem. Phys. Meteorol.*, 65, <https://doi.org/10.3402/tellusb.v65i0.20480>, 2013.
- 543 Wedin, D. A. and Tilman, D.: Influence of nitrogen loading and species composition on the carbon balance of
544 grasslands, *Science*, 274, <https://doi.org/10.1126/science.274.5293.1720>, 1996.
- 545 Wu, L., Ren, H., Wang, P., Chen, J., Fang, Y., Hu, W., Ren, L., Deng, J., Song, Y., Li, J., Sun, Y., Wang, Z., Liu,
546 C.-Q., Ying, Q., and Fu, P.: Aerosol ammonium in the urban boundary layer in Beijing: insights from nitrogen
547 isotope ratios and simulations in summer 2015, *Environ. Sci. Technol. Lett.*, 6, 389-395,
548 <https://doi.org/10.1021/acs.estlett.9b00328>, 2019.
- 549 Xiang, Y.-K., Dao, X., Gao, M., Lin, Y.-C., Cao, F., Yang, X.-Y., and Zhang, Y.-L.: Nitrogen isotope characteristics
550 and source apportionment of atmospheric ammonium in urban cities during a haze event in Northern China
551 Plain, *Atmos. Environ.*, 269, 118800, <https://doi.org/10.1016/j.atmosenv.2021.118800>, 2022.
- 552 Xiao, H. W., Wu, J. F., Luo, L., Liu, C., Xie, Y. J., and Xiao, H. Y.: Enhanced biomass burning as a source of
553 aerosol ammonium over cities in central China in autumn, *Environ. Pollut.*, 266, 115278,
554 <https://doi.org/10.1016/j.envpol.2020.115278>, 2020.
- 555 Yang, Y., Li, P., He, H., Zhao, X., Datta, A., Ma, W., Zhang, Y., Liu, X., Han, W., Wilson, M. C., and Fang, J.:
556 Long-term changes in soil pH across major forest ecosystems in China, *Geophys. Res. Lett.*, 42, 933-940,
557 <https://doi.org/10.1002/2014gl062575>, 2015.
- 558 Yu, X., Shen, L., Hou, X., Yuan, L., Pan, Y., An, J., and Yan, S.: High-resolution anthropogenic ammonia emission
559 inventory for the Yangtze River Delta, China, *Chemosphere*, 251, 126342,
560 <https://doi.org/10.1016/j.chemosphere.2020.126342>, 2020.
- 561 Zhang, Z., Zeng, Y., Zheng, N., Luo, L., Xiao, H., and Xiao, H.: Fossil fuel-related emissions were the major
562 source of NH₃ pollution in urban cities of northern China in the autumn of 2017, *Environ. Pollut.*, 256, 113428,
563 <https://doi.org/10.1016/j.envpol.2019.113428>, 2020.
- 564 Zhang, Z., Zhu, W., Hu, M., Wang, H., Tang, L., Hu, S., Shen, R., Yu, Y., Song, K., Tan, R., Chen, Z., Chen, S.,
565 Canonaco, F., Prevot, A. S. H., and Guo, S.: Secondary organic aerosol formation in China from urban-lifestyle
566 sources: Vehicle exhaust and cooking emission, *Sci. Total Environ.*, 857, 159340,
567 <https://doi.org/10.1016/j.scitotenv.2022.159340>, 2022.
- 568 Zhao, Y., Tkacik, D. S., May, A. A., Donahue, N. M., and Robinson, A. L.: Mobile sources are still an important
569 source of secondary organic aerosol and fine particulate matter in the los angeles region, *Environ. Sci. Technol.*,
570 56, 15328-15336, <https://doi.org/10.1021/acs.est.2c03317>, 2022a.
- 571 Zhao, Y., Xi, M., Zhang, Q., Dong, Z., Ma, M., Zhou, K., Xu, W., Xing, J., Zheng, B., Wen, Z., Liu, X., Nielsen,
572 C. P., Liu, Y., Pan, Y., and Zhang, L.: Decline in bulk deposition of air pollutants in China lags behind reductions
573 in emissions, *Nat. Geosci.*, 15, 190-195, <https://doi.org/10.1038/s41561-022-00899-1>, 2022b.
- 574 Zheng, L., Chen, W., Jia, S., Wu, L., Zhong, B., Liao, W., Chang, M., Wang, W., and Wang, X.: Temporal and



- 575 spatial patterns of nitrogen wet deposition in different weather types in the Pearl River Delta (PRD), China, *Sci.*
576 *Total Environ.*, 740, 139936, <https://doi.org/10.1016/j.scitotenv.2020.139936>, 2020.
- 577 Zhu, J., He, N., Wang, Q., Yuan, G., Wen, D., Yu, G., and Jia, Y.: The composition, spatial patterns, and influencing
578 factors of atmospheric wet nitrogen deposition in Chinese terrestrial ecosystems, *Sci. Total Environ.*, 511, 777-
579 785, <https://doi.org/10.1016/j.scitotenv.2014.12.038>, 2015.
- 580 Zong, Z., Tan, Y., Wang, X., Tian, C., Li, J., Fang, Y., Chen, Y., Cui, S., and Zhang, G.: Dual-modelling-based
581 source apportionment of NO_x in five Chinese megacities: providing the isotopic footprint from 2013 to 2014,
582 *Environ. Int.*, 137, 105592, <https://doi.org/10.1016/j.envint.2020.105592>, 2020.
- 583 Zong, Z., Wang, X., Tian, C., Chen, Y., Fang, Y., Zhang, F., Li, C., Sun, J., Li, J., and Zhang, G.: First assessment
584 of NO_x sources at a regional background site in North China using isotopic analysis linked with modeling,
585 *Environ. Sci. Technol.*, 51, 5923-5931, <https://doi.org/10.1021/acs.est.6b06316>, 2017.
- 586